Identification of Volcanic Breccia Formation Distribution in Relation to Groundwater Potential Using 3D Resistivity Data Modelling

H E H Fatahillah[1]*, P N Ratna[2], F Septiawan[1], R N Pratama[1], M R A Ghiffari[1], N Wicaksono[1], W Hidayat[1], M R Noor[1] and R Ramadhan[1]

[1]*Pusat Riset Teknologi Pertambangan, Organisasi Riset Nanoteknologi dan Material, Badan Riset dan Inovasi Nasional, Gedung 820 Kawasan Puspiptek, Serpong, Tangerang Selatan, Banten, Indonesia 15314*
[2]*Pusat Riset Kebencanaan Geologi, Organisasi Riset Kebumian dan Maritim, Badan Riset dan Inovasi Nasional, Kawasan Bandung Cisitu Jalan Sangkuriang, Dago, Kecamatan Coblong, Kota Bandung, Jawa Barat, Indonesia 40135*

**Corresponding author's email: hilm006@brin.go.id*

Abstract. Electrical resistivity tomography (ERT) method has been widely used in environmental surveys including hydrogeology study to provide images of the subsurface resistivity distribution. In this study, ERT survey using Wenner - Schlumberger electrode configuration was conducted to investigate the distribution of aquifer potential in the area dominated by various weathered volcanic rocks that unconformably overlaid limestone formation. The resistivities were measured using ARES resistivity meter each with total of 48 electrodes. The resistivity data were then processed using the robust inversion method that is more optimal to characterize sharp lithological boundary transitions observed in the study area. The resistivity value of the inverted model is interpreted into three different lithologies, namely soil (1.82-5 Ωm), volcanic breccias (5-20 Ωm) and limestone (>20 Ωm). This lithological interpretation was confirmed by borehole cutting report from the nearby well, regional geological map, and direct geological observation. Further, the inverted ERT section along with geological observation indicated volcanic breccias as an aquifer potential in the study area. The 2D resistivity cross-section is then gridded to obtain a 3D model of the aquifer geometry. From the model, the volume of volcanic breccia which is suspected as an aquifer layer is estimated at 122,392,828 m^3.

Keywords: resistivity, electrical resistivity tomography, Wenner-Schlumberger, robust inversion, groundwater, 3D modelling

1. Introduction

Water is an absolute necessity for the survival of humans, animals, and plants. Almost all daily human activities require water as a basic material and as a supporting material, including in the industrial and agricultural fields. The water source could be found beneath the ground and often called groundwater. The role of geophysics is very necessary to investigate the subsurface condition of a rock layer in order to look for potential groundwater aquifers. Electrical resistivity tomography (ERT) is one of the commonly used geophysical methods to map subsurface electrical resistivity [1,2] and helped to delineate subsurface geological structures, formations, and aquifer zones [3]. The depth of occurrence of groundwater zones can also be determined more effectively by this method [4]

Electrical resistivity tomography (ERT) measures the electrical properties of the subsurface material based on the resistivity value of the material by injecting an electric current and measuring its potential on the surface. The basic principle of the ERT method is to use the resistivity value as a differentiator between lithologies by assuming that the differences in physical properties in each type of lithology will result in different resistivity values. The measurement of subsurface mapping using ERT is taken by injecting electric current (I) (in mA units) into the earth through two current electrodes. Later, the potential difference (V) that occurs (in units of mV) due to current injection is measured through two potential electrodes.

Study area is located in the area dominated by thick layer of various weathered volcanic rocks that overlies limestone (Tmv formation) as shown by regional geological map (figure 1) and direct geological observation. The weathered characteristic in the volcanic rocks potentially increases the porosity within the rock and eventually also increases the quality of the rock as an aquifer potential.

In this study, we carried out an ERT survey using Wenner-Schlumberger configuration with 14 measurement lines and 3D modelling to investigate the geometry and the volume of volcanic breccia as the aquifer potential in the study area.

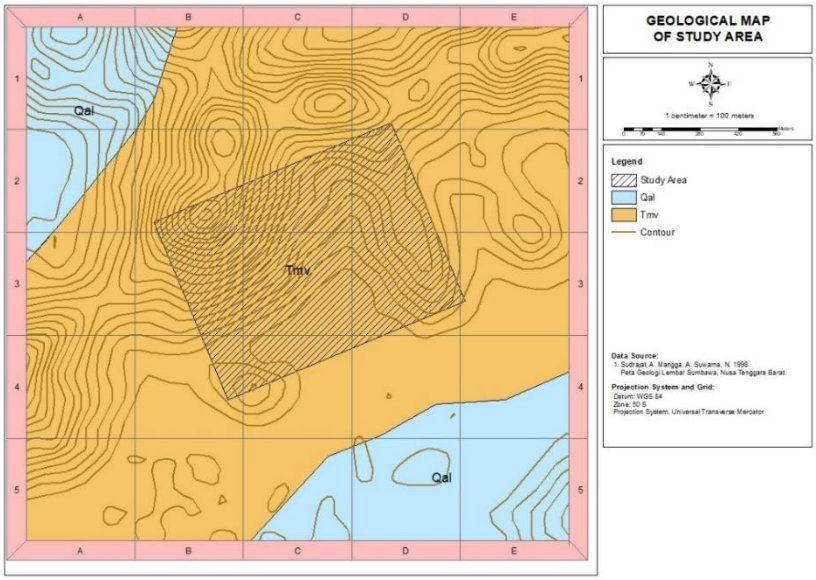

Figure 1. Geological map of the study area.

2. Data and Methodology

2.1. Geological setting

The regional geological map of the study area can be seen in figure 1. It consists of two rock units, namely Qal and Tmv [5]. Qal unit is a quaternary alluvial and coastal deposit that is composed of gravels, sands, clay, mud, and beach sands. It mainly comprises andesitic material and locally contains magnetite. This unit is spread along the north and south coasts. Meanwhile, the Tmv unit is a tuff-breccia unit of the early Miocene - middle Miocene age. Breccia is characterized as andesitic, with sandy tuff, pumiceous tuff, and tuffaceous sandstone, locally containing lahar and andesitic and basaltic lavas. Generally, Tmv unit is greenish-grey and green in color. It also has pillow-structured lava with chert intercalation. The rock unit is propylitised, mineralized, and silicified locally, with quartz and calcite veins. This tuff-breccia unit interfingers with the Tuffaceous Sandstone Units (Tms) and Limestone Units (Tml). In addition, this Tmv unit also underlies the Coralline Limestone (Tmcl) unit unconformably. Its distribution can be found in the south of the island, extending from west to east.

2.2. Borehole cuttings report

In this present study, borehole cuttings report from the nearby well, along with direct geological observation, were used to validate the ERT interpretation results. Based on the observation, these cuttings can be classified into three parts: upper, middle, and lower part. The upper part (0-18m depth) which is soft and light to dark brown in color, is associated with soil. The hard and greenish-grey cuttings from the middle part (18-64m depth) indicate volcanic breccia that was found in the area. Then, the lower part (64-141m depth) shows hard and broken white cuttings that is interpreted as limestone.

2.3. Survey design

In this study area, Electrical Resistivity Tomography (ERT) survey was conducted using 48 electrodes which connected using multi-electrode cable with ARES Resistivity Meter (GF Instrument). The survey was performed using Wenner-Schlumberger configuration. This array has a moderate depth of investigation and strong signal strength, which permits to be relatively sensitive to vertical and horizontal variations in the subsurface [6].

There were two measurement directions applied, the northwest-southeast (NW-SE) and the southwest-northeast (SW-NE) (figure 2). The NW-SE consists of five measurement trajectories. It has a distance between each trajectory about 175 m and a spacing between electrodes within a line of 15 m. Meanwhile, the SW-NE consists of nine measurement trajectories. It has irregular distances between each measurement line which ranges from 35m - 85m and a spacing between electrodes within a line of 20 m to avoid contact with existing infrastructures.

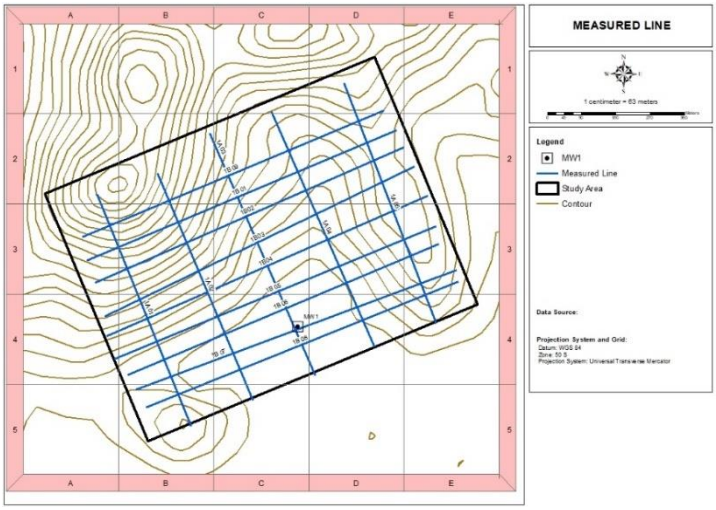

Figure 2. ERT measured line.

2.4. Inversion

In order to obtain earth model of the area under the investigated ERT line, resistivity data are inverted. This method is applied to determine a subsurface model whose response agrees with the measured data. A frequently used inversion technique for 2D or 3D ERT inversion is L2 norm or smoothness-constrained least-squares optimization [7]. This method minimizes the sum the squares of the misfit data, so it will give optimal results where the subsurface geology of the area shows a smooth variation. However, when there is a sharp transition on the subsurface, this method tends to make boundaries between the subsurface smeared. As a substitute method, robust inversion or L1 norm optimization is used that minimizes the sum of the absolute values of the data misfit. It tends to produce models with sharp interfaces between regions with different resistivity values, but in each region, the resistivity value is almost constant [8,9]. The procedure to implement L1 norm using the standard least-squares formulation is iteratively re-weighted smoothness-constrained least-squares (IRLS) method for the data inversion as in question (1) [10,11].

$$\left(J_i^T G_d J_i + \varepsilon_i W^T G_m W\right)\Delta r_i = J_i^T G_d e_i - \varepsilon_i W^T G_m W r_{i-1} \quad (1)$$

where e_i is the data misfit vector comprising the difference between the measured and calculated apparent resistivity values, Δr_i is the change in the model parameters for the ith iteration and r_{i-1} is the model parameters vector for the previous iteration. J is the Jacobian matrix of partial derivatives and W is the roughness filter [12]. The damping factor, ε, determines the relative importance given to minimizing the model roughness. G_d and G_m are two weighting diagonal matrices introduced so that different elements of the data misfit and model roughness vectors are given approximately equal weights in the inversion process. A more detailed explanation of the inversion method is given in [7].

3. Results and Discussion

The ERT data is processed using RES2DINV and 3D Modelling Software. The resistivity data from fourteen lines were inverted using robust inversion methods and normal spacing parameter with cut off value of 0.1. The 2D inverted ERT models of each line obtained after five iterations and resulted in lowest root mean square error value ranging from 1.7% to 5.9%. Resistivity values resulted from the inversion process varied from 1.82 Ωm up to more than 135 Ωm. Topographical correction process also applied to each model to bring up resistivity datum to the correct depth. In order to create a comparable resistivity model from each ERT line, the distribution of resistivity values was displayed using a fixed and unified color scale for all models.

The nine inverted models from the SW-NE measurement line provided a deeper subsurface resistivity image than the rest of the models resulted from measurement line with perpendicular direction as shown in figure 3. The difference in the depth of subsurface resistivity images occurred because the electrode spacing of the measurement line with the southwest-northeast direction is wider than the spacing in the line of northwest-southeast direction, 20-meter and 15-meter electrode spacing, respectively.

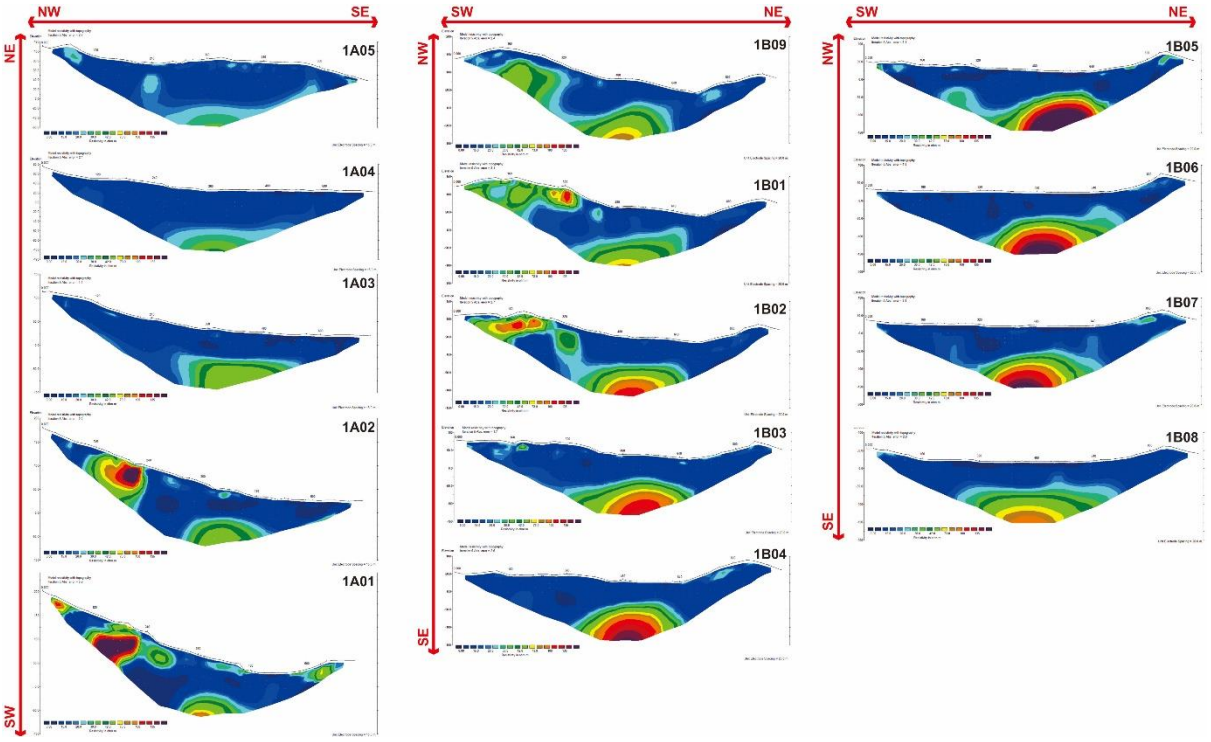

Figure 3. 2D inverted ERT models from 14 measured ERT lines.

The resistivity value from the inverted models of fourteen ERT lines can be divided into two types of anomalies. The first anomaly is the low resistivity value ranging from 1.82-20 Ωm that dominates the upper area of all models. The second one is the high resistivity anomaly (>20 Ωm). This high resistivity anomaly appears in the lower part of all lines, southwestern part of line 1B02 and 1B03, and northwestern part of line 1A01 and 1A02.

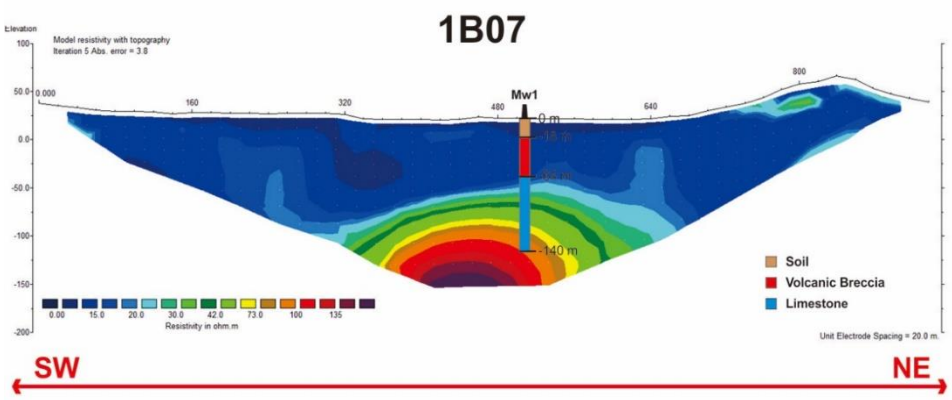

Figure 4. Correlation between inverted ERT model line 1B07 with geological cuttings report.

The low resistivity anomaly in the study area is interpreted as the resistivity response from wet soil (1.82 to 5 Ωm) and volcanic breccia (5-20 Ωm). Meanwhile, the high resistivity anomaly is defined as limestone resistivity response. This interpretation is based on correlation with geological cutting reports, regional geology information (figure 1), geological observations (figure 5), and literature reference of rock resistivity value (table 1). The correlation between geological cutting reports and inverted cross section model from line 1B07 shows that low resistivity value is correlated to soil (0-18 m depth) and cuttings that is associated with volcanic breccia observed in the study area (18-64 m depth). Meanwhile, the high resistivity value is correlated to limestone cuttings from the depth of 64 to 141 m (figure 4). Regionally (figure 1), the volcanic breccia and limestone unit identified in the study area is the part of Tuff-Breccia Unit (Tmv) that interfingers with Limestone Unit (Tml) and in some regions, unconformably underlies Coraline Limestone Unit (Tmcl). There are slight differences between

references and measured resistivity value of volcanic breccia and limestone in the study area where the measured value tends to show lower ranges of resistivity value than the theoretical one (table 1). The difference in this resistivity value may occur due to different geological conditions. Weathered rock condition and water content in the study area may bring down the resistivity value of the lithology. Further, the low resistivity of volcanic breccia may occur because the breccia found in the study area is matrix-dominated which the matrix is composed by tuff (figure 5). The presence of tuff as a matrix potentially reduces the resistivity value of the volcanic breccia due to its low resistivity (5-14 Ωm).

Table 1. Comparisson between reference and measured resistivity value [13,14,15]

Lithology	Reference resistivity value (Ωm)	Measured Resistivity Value (Ωm)
Soil	2.4-18	1.82-5
Volcanic Breccia	90-290	5-20
Limestone	50-10^7	>20
Tuff	5-14	-

The inverted ERT model and the geological information suggest that volcanic breccia is a better aquifer potential than the limestone. The volcanic breccia in the study area is matrix-dominated with a coarse tuff arrangement providing good porosity and permeability as a groundwater aquifer. It also has lower resistivity value than that of limestone which may indicate a higher water-saturation within the rock body. Furthermore, groundwater extracted from non-carbonate aquifer tends have a lower total dissolved solid (TDS) than carbonate aquifer [16].

Figure 5. Volcanic breccia outcrop in the study area.

The 2D cross-section of resistivity models then gridded using nearest neighbor interpolation to obtain 3D resistivity models (figure 6(a)). The resistivity value on the 3D resistivity models then grouped based on the interpretation of the resistivity value to generate 3D lithological models (figure 6(b)). Qualitative analysis is used to analyze the subsurface lithological distribution and reservoir geometry. Meanwhile, quantitative analysis is applied to calculate the volume of volcanic breccia as an aquifer.

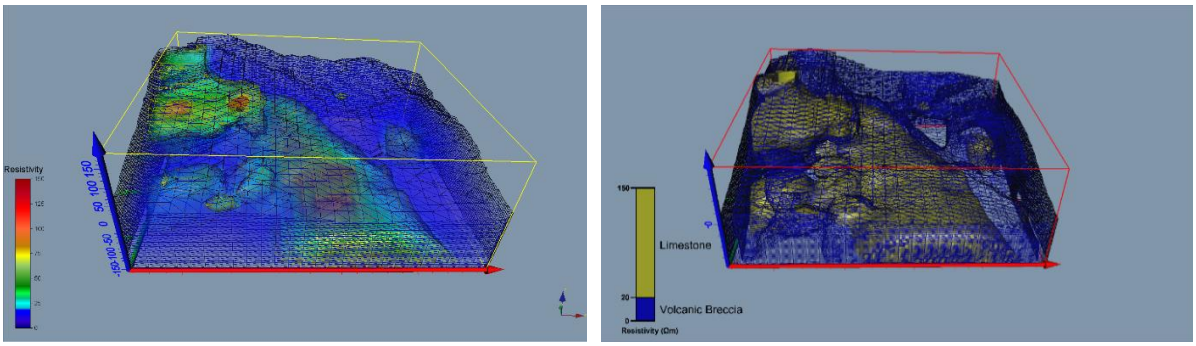

(a) (b)

Figure 6. (a) 3D resistivity model, (b) 3D lithological model

In the 3D lithological model, volcanic breccia is represented by blue color and limestone is shown by yellow color. The model shows that volcanic breccia is distributed in the entire upper part of the study area. The thickest layer of volcanic breccia is found in the western part of the study area, while the thinnest layer is in the middle to the eastern part. Meanwhile, limestone can be discovered below the

layer of volcanic breccia. The thickest layer of limestone in the middle part of study area, extending from south to the northwest. Based on the 3D model calculations, the volume of volcanic breccia is calculated at 122,392,828 m^3.

4. Conclusions

To conclude, this study area is composed by volcanic rock formations that overlies limestone. ERT method has been proved to be able to locate groundwater potential that is also confirmed by a nearby well. The resistivity value is interpreted as soil (1.82 – 5 Ωm), volcanic breccia (5 – 20 Ωm), and limestone (>20 Ωm). Furthermore, the volcanic breccia is considered as the preferred groundwater aquifer potential because it shows more graded characteristic due to its presumed better porosity. The 3D model suggests that the volume of volcanic breccia reaches 122,392,828 m^3.

References

[1] Dahlin T 2001 The development of DC resistivity imaging techniques Computers and Geosciences 27(9) 1019– 29
[2] Griffiths D H and Barker R D 1993 Two-dimensional resistivity imaging and modelling of areas of complex geology *Journal of Applied Geophysics* **29**(3–4) 211–26 doi:10.1016/0926-9851(93)90005-j
[3] Azffri S L, Ibrahim M F and Gödeke S H 2022 Electrical resistivity tomography and induced polarization study for groundwater exploration in the agricultural development areas of Brunei Darussalam *Environmental Earth Sciences*\ **81**(8) 1–12 doi: 10.1007/s12665-022-10284-1
[4] Bharti A K, Pal S K, Saurabh, Singh K K K, Singh P K, Prakash A and Tiwary R K 2019 Groundwater prospecting by the inversion of cumulative data of Wenner–Schlumberger and dipole–dipole arrays: A case study at Turamdih, Jharkhand, India *Journal of Earth System Science* **128**(4) 1–10 doi: 10.1007/s12040-019-1137-2
[5] Sudradjat A, Mangga S.A, and Suwarna N 1998 Geological Map of the Sumbawa Quadrangle Nusatenggara
[6] Loke M H 2021 Tutorial: 2-D and 3-D electrical Imaging Surveys
[7] Loke M H, Acworth I and Dahlin T 2003 A comparison of smooth and blocky inversion methods in 2D electrical imaging surveys *Exploration Geophysics* **34**(3) 182–187 doi: 10.1071/EG03182
[8] Al-Amoush H, Rajab J, Al-Tarazi E, Alshabeeb A R, Al-Adamat R and Al Fugara A 2017 Electrical Resistivity Tomography Modeling of Vertical Lithological Contact using Different Electrode Configurations *Jordan Journal of Earth and Environmental Sciences*, **8**(1) 27–34
[9] Lysdahl A K, Bazin S, Christensen C, Ahrens S, Günther T and Pfaffhuber A A 2017 Comparison between 2D and 3D ERT inversion for engineering site investigations - A case study from Oslo Harbour *Near Surface Geophysics* **15**(2) 201–209 doi: 10.3997/1873-0604.2016052
[10] Farquharson C G and Oldenburg D W 1998 Non-linear inversion using general measures of data misfit and model structure Geophysical Journal International 134(1) 213–227 doi: 10.1046/j.1365-246x.1998.00555.x
[11] Wolke R and Schwetlick H 1988 Iteratively reweighted least squares algorithms, convergence analysis, and numerical comparisons *SIAM Journal of Scientific and Statistical Computations* **9** 907–921 doi: 10.1137/0909062
[12] Degroot-Hedlin C and Constable S 1990 Occam's inversion to generate smooth, two-dimensional models from magnetotelluric data *Geophysics* **55**(12) 1613–1624 doi: 10.1190/1.1442813
[13] Ayolabi E A, Adetayo F and Olubunmi J 2012 An application of 2D electrical resistivity tomography in geotechnical investigations of foundation defects: A case study Journal of Geology and Mining Research 3(12) 142–51 doi: 10.5897/JGMR12.002
[14] Manyoe I N and Hutagalung R 2020 Subsurface Shallow Modelling Based on Resistivity Data in The Hot Springs Area of Libungo Geothermal, Gorontalo *Journal of Geoscience, Engineering, Environment, and Technology* **5**(2) 87–93 doi: 10.25299/jgeet.2020.5.2.5094
[15] Telford W M, Geldart L P and Sheriff R E 1990 *Applied Geophysics 2nd Edition* (Cambridge: University Press Cambridge) p 290
[16] Jacobson R L and Langmuir D 1974 Controls on the quality variations of some carbonate spring waters *Journal of Hydrology* **23**(3–4) 247–65 doi: 10.1016/0022-1694(74)90006-7